Discretization-Based Analysis of Structural Electrodynamics

Soo-Joon Kang* and Ki-Soon Park**

(*Received June 25, 1999*)

This paper experimentally confirms the fundamental dynamic properties of an electrodynamic structure. The discretization effects are examined for the conversion of continuous properties such as mass, stiffness and surface charge into discrete quantities. In the systems considered, the linearized characteristics are well-matched with the nonlinear systems in the sense that the linearized effects dominate over the high-order nonlinear terms. A conductive strip experiment is conducted in order to improve our understanding of the fundamental characteristics of the electrodynamic structure from discrete systems to continuous systems. The measured equilibrium positions agree with the analytically predicted equilibrium positions up to some small errors.

Key Words: Structural Electrodynamics, Discretization Effect, Discrete System, Linearized Effect, Conductive Strip, Equilibrium Position

1. Introduction

This paper considers structures whose dynamic characteristics are predominantly derived from external free-electron forces. These structures will be referred to as electrodynamic structures, and the study of such systems will be referred to as structural electrodynamics. No known fundamental studies in structural electrodynamics were found in the searched literature, although specific applications utilizing the electrostatic forces have been reported (Park, 1992; Bryant et al., 1986; Rhim et al., 1985; Udd, 1985; Mihora et al., 1979; Brook et al., 1982; Golsee et al., 1985; Kang et al., 1999). The electrostatic form of thin film membranes has been proposed (Mihora et al., 1979), in which nonlinear large-deflection membranes are considered for use as optical reflectors. In other investigations, a large antenna concept has been studied by NASA (Brook et al., 1982). The antenna was designed and fabricated with flat and curved back electrodes. This research suggests that surface charges, when appropriately controlled, can be turned from a liability into an asset. Potential benefits include reduction of thermally induced mechanical stresses caused by thermal gradients, reduced warping, elimination of moving mechanical components, and varying equilibrium position capability (deployment, slewing, uncoiling, varying focal length, etc.) (Grohe, 1960; Lewis, 1985; Giachino, 1986; Kind et al., 1985; Doggett et al., 1990; Quinn, 1985; Wada, 1989; Chong et al., 1990; Wen, 1992; Golsee et al., 1985). The technology is applicable to precise surfaces (lenses, mirrors, microwave/optical antennas, reflectors, acoustical membranes, micromotors, linear force actuators, etc.). The fundamental properties (static equilibrium angles and natural frequencies) of the electrically charged particle motion is investigated analytically (Kang et al., 1999a). By adopting a discrete particles approach, Kang and Park formulate the equations governing the planar electrodynamics of interconnected electrical charged particles. Then, as simple examples, they describe the electrodynamics of the fixed charge electroscope and the electrostatic string (Kang et al., 1999b).

In this paper the discretization effects are examined for the conversion of continuous properties such as mass, stiffness and surface charge

* Department of Mechanical Engineering, Republic of Korea Air Force Academy, 363-849, Korea.
** HQ, Republic of Korea Air Force, 320-919, Korea.

into discrete quantities. The material properties are measured to account for stiffness effects, and for boundary effects with grounded materials which are investigated to seek efficient methods to get a larger value of strip deflections using appropriate voltages. In this paper, an experiment for a conductive strip is conducted in order to improve our understanding of the discretization-based analysis of structural electrodynamics.

2. Formulations

2.1 Electrostatic potential energy (Halliday et. al, 1970)

The work done on a test charge Q' by the electric field $\vec{E}$ during an arbitrary displacement from point a to point b, as shown in Fig. 1, is given by

$$W_{ab}=\int_a^b \vec{F}\cdot d\vec{s}=\int_a^b Q'\vec{E}\cdot d\vec{s}=Q'\int_a^b E\cos\theta ds$$
$$=\chi QQ'\int_{r_a}^{r_b}\frac{dr}{r}=\chi QQ'\left(\frac{1}{r_a}-\frac{1}{r_b}\right)$$
$$=(U_e)_a-(U_e)_b \qquad (1)$$

in which Q' and Q denote a test charge which is moving along an arbitrary path from a to b, and a fixed charge in the electric field, respectively. $\vec{E}$ is an electric field vector whose magnitude, the electric field strength E, is $\frac{\chi Q}{r^2}$, where r is the distance from the measured position to Q. Here χ denotes the electrical constant of the medium which is $\chi=8.98755\times10^9\approx9\times10^9(\mathrm{N}\,m^2\,C^{-2})$, ε_0 is the permittivity of the free space given by $\varepsilon_0\cong 8.854\times10^{-12}$ (F/m). $(U_e)_a$, and $(U_e)_b$ denotes the electric potential energy at points a and b, respectively.

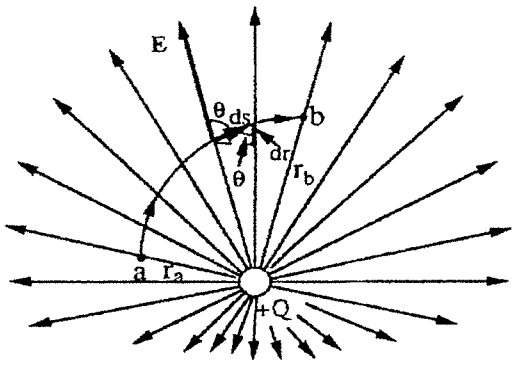

Fig. 1 Electric field ($\vec{E}$) system.

Equation (1) identifies the work done on a test charge Q' by the electric field $\vec{E}$, which depends only on the initial distance r_a (a distance from a fixed charge Q to a point a) and the final distance r_b (a distance from a fixed charge Q to a point b), and not on the path connecting these points a and b. The work done by a conservative force can be represented by a potential energy function. We may consider the distance r_a to define the base reference level from which the potential energy is measured. It is often convenient to let point a be at an infinite distance, that is, letting $r_a=\infty$, so that $(U_e)_a=(U_e)_\infty=0$. Thus, the potential energy of the test charge at any point in an electric field is equal to the work done by the electric force when the test charge is brought from the point in question to a reference level, often taken as infinity.

From the above ideas, to bring a charge q_2 from an infinite distance against the field of a charge q_1 to a distance r_{12} requires work which is equal to the final potential energy

$$(U_e)_2=\frac{\chi q_1q_2}{r_{12}} \qquad (2)$$

Now suppose another charge q_3 is brought from an infinite distance to a point that is r_{13} from q_1 and r_{23} from q_2. The total potential energy then is

$$(U_e)_3=(U_e)_2+\frac{\chi q_1q_3}{r_{13}}+\frac{\chi q_2q_3}{r_{23}} \qquad (3)$$

Extending this procedure to additional charges, we arrive at the following general expression for the potential energy of a group of n discrete point charges at rest. The general form is given by

$$(U_e)_n=\sum_{i=1}^{n-1}\sum_{j=i+1}^{n}\frac{\chi q_iq_j}{r_{ij}}=\frac{1}{2}\sum_{i=1}^{n}\sum_{j=1,i\neq j}^{n}\frac{\chi q_iq_j}{r_{ij}}$$
$$=\frac{1}{2}\sum_{i=1}^{n}\sum_{j=1,i\neq j}^{n}\frac{\chi q_iq_j}{|\vec{r}_i-\vec{r}_j|} \qquad (4)$$

in which $r_i(i=1,2,\cdots,n)$ and $r_j(j=1,2,\cdots,n)$ denote the distance of the i-th fixed charge from the reference and the distance of the j-th fixed charge from the reference point, respectively.

2.2 Discretization of the structure

Consider a cantilever beam with uniformly

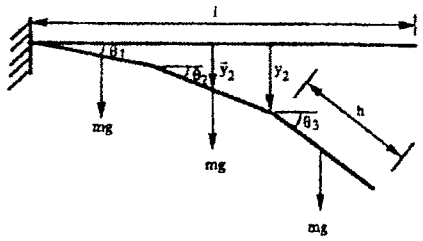

Fig. 2 Discrete cantilever beam.

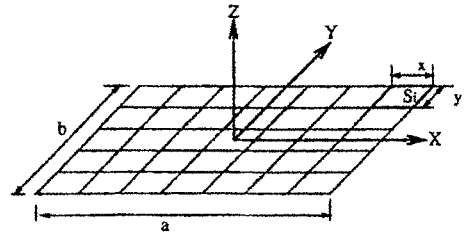

Fig. 3 Rectangular conducting plate and subdomains.

distributed loads. The beam has a distributed mass and stiffness. The strain energy of the beam (Meirovitch, 1980) is

$$U_s=\frac{1}{2}\int_0^l EI(x)\left(\frac{d^2y}{dx^2}\right)^2 dx \tag{5}$$

in which E and $I(x)$ denote the elastic modulus and the moment of inertia, respectively, and l and y denote the length of the beam and the transverse displacement of the beam, respectively. The beam is now discretized into n elements of width h as shown in Fig. 2, where $nh=l$, and the mass associated with these segments is lumped into discrete masses at the center of the segments. The angles of rotation are measured relative to the horizontal axis.

From Fig. 2,

$$\frac{d^2y}{dx^2}\approx\frac{\theta_i-\theta_{i-1}}{h},\ (ih<x<(i+1)h) \tag{6}$$

where θ_i denotes the angle of rotation at $x=ih$. Note that Eq. (5) and (6) assume small curvature; however, the displacements and slopes can be large. Indeed, discretization by Eq. (6) allows for a beam that is undergoing large deformations. Substituting Eq. (6) into (5), the strain energy for the discrete system can be expressed as a function of the generalized coordinates as follows:

$$\begin{aligned}U_s&=\frac{1}{2}\sum_{i=1}^{n}\frac{EI}{h}(\theta_i-\theta_{i-1})^2\\&=\frac{1}{2}\sum_{i=1}^{n}\sum_{j=1}^{n}k_{ij}^{s}\theta_i\theta_j\ (\theta_0=0)\end{aligned} \tag{7}$$

in which

$$[k_{ij}^{s}]=\frac{EI}{h}\begin{bmatrix}2&-1&0&0&\cdots&0\\-1&2&-1&0&\cdots&\vdots\\0&-1&2&-1&&\\\vdots&&&&&0\\0&\cdots&&0&\cdots&\vdots\end{bmatrix}_{n\times n} \tag{8}$$

2.3 Discretization of the charge

The exact solution for the charge distribution can be obtained only for a few specialized geometries. In general, the surface must be discretized, and the distributions are found by a numerical method. A numerical method to calculate the charge distributions over a square subdomain is introduced (in Harrington, 1968).

Consider a rectangular plate of dimension $a\times b$, perfectly conducted by a potential V, which is divided into n identical rectangular subdomains as shown in Fig. 3. In Fig. 3, $S_i(=x\times y)$ represents the area of the i-th subdomain, and Q_i represents the charge over the i-th subdomain. The potential V_i (on the i-th subdomain) is due to its own charge and to the charges on the other subdomains. The procedure yields a set of n linear algebraic equations in terms of n unknown charges:

$$V_i=\sum_{j=1}^{n}P_{ij}Q_j\ (j=1,\ 2,\ \cdots,\ n) \tag{9}$$

where $P_{ij}(i,\ j=1,\ 2,\ \cdots,\ n)$, are called the coefficients of potential.

In the planar case, P_{ij} is given by

$$P_{ij}\approx\frac{x}{\sqrt{(x_j-x_i)^2+(y_j-y_i)^2}},\ (i\neq j) \tag{10}$$

where the position $(x_i,\ y_i)$ refers to the center of the i-th subdomain.

The inversion of Eq. (9) yields the surface charge over each subdomain. Since the potential of a conductor is distributed uniformly over its surface, we let the potential V_i be equal to V. The capacitance of the rectangular plate is then given by

$$C=\frac{Q}{V}\approx\frac{1}{V}\sum_{i=1}^{n}Q_i \tag{11}$$

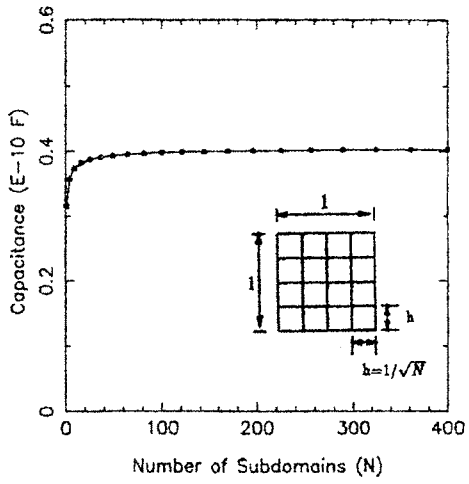

Fig. 4 Capacitance as a function of the subdomains.

where Q and n denote the total electric charges and the number of the subdomain, respectively.

Figure 4 shows the capacitance as a function of the number of the subdomain. It shows that the charge distributions are almost constant when the number of subdomains is greater than 100. In general, charge densities along the edges of the plate are greater than the charge densities adjacent to the centerline of the plate (Rao, et al., 1979).

2.4 Static equilibrium equation

Invoking Lagrange's equations of motion for conservative systems, we obtain a set of nonlinear ordinary differential equations in general coordinates $\hat{q}_i (i=1, 2, \cdots, n)$ as follows (Meirovitch, 1970):

$$0=\frac{d}{dt}\left[\frac{\partial T}{\partial \dot{\hat{q}}_i}\right]-\frac{\partial T}{\partial \hat{q}_i}+\frac{\partial U}{\partial \hat{q}_i}, \quad (i=1, 2, \cdots, n) \quad (12)$$

in which T and U denote the kinetic energy and the potential energy, respectively.

From Eq. (12), neglecting the gravitational energy in this system, the potential energy of the system can only be composed of the electrical energy U_e and strain energy U_s, by carrying out the necessary differentiations, and letting the acceleration and velocity terms equal zero, that is, $\dot{\hat{q}}_i(t)=\ddot{\hat{q}}_i(t)=0$ $(k=1, 2, \cdots, n)$, we obtain the nonlinear set of algebraic equations governing the static equilibrium of the planar electrodynamic

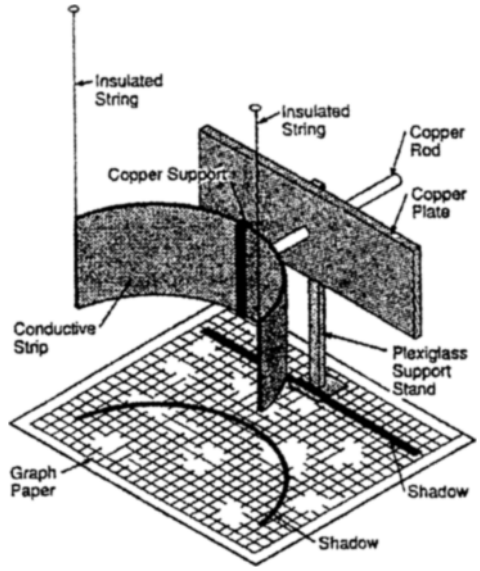

Fig. 5 Conductive strip experimental system.

system as follows:

$$\frac{\partial U}{\partial \hat{q}_l^o}=-\sum_{i=1}^{n-1}\sum_{j=i+1}^{n}\frac{xq_iq_j}{|\hat{q}_i^o-\hat{q}_j^o|^2}\cdot\frac{\partial}{\partial \hat{q}_l^o}|\hat{q}_i^o-\hat{q}_j^o| + \sum_{i=1}^{n}k_{li}^s\hat{q}_i^o=0 \quad (l=1, 2, \cdots, n) \quad (13)$$

in which $\hat{q}_j^o$ denotes the equilibrium position and k_{ij}^s is Eq. (8).

3. Experiment and Results

3.1 Laboratory set up

The objective of the continuous conductive strip experiment is to improve our understanding of structural electrodynamics from discrete systems to continuous systems. The specific purpose of the experiment is to measure the equilibrium positions of the continuous conductive strip. In the experimental system, a thin conductive strip is electrically connected to a copper plate as shown in Fig. 5.

The thin fabric strip is made of 100% polyester non-woven interfacing sheet, which is coated with a conductive material, Aquadag-E, which has a low mass, low stiffness, and a smooth surface.

The experimental system is designed to generate electric fields that cause repelling forces between the conductive strip and the rigid copper plate. As

shown in Fig. 5, a conductive strip of dimension (304.8 mm×63.5 mm is fixed at the end of the copper rod of length (101.6 mm), and suspended simultaneously at the end of both side by two insulated strings. A copper plate of dimension (304.8 mm×76.2 mm is also fixed to the plexiglass supporting stand. The conductive strip and the copper plate are electrically connected to a common power supply providing a maximum voltage of 30 kilovolts. The position of the conductive strip must be adjusted after each measurement to its original position using strings for the sequential experiments. The equilibrium position of the strip is measured from a shadow created by the strip casting on the grid paper (the grid is composed of 1.27 mm×1.27 mm squares). The measurements are first videotaped and then evaluated.

3.2 Measurements of the flexural rigidity of the strip

In order to account for the stiffness effect of the conductive strip, the effective flexural rigidity $\bar{E}I$ is measured. The weight of the conductive strip coated with the conductive material Aquadag-E is 0.277 N/m^2(0.227 N/m^2 before coating). The cantilevered strip deforms under its own weight. The measured deflections at the free end of the conductive strip are shown in Fig. 6. Table 1 shows that the measured effective flexural rigidity of the strip is 0.425×10^{-6} kg.m^3/sec^2.

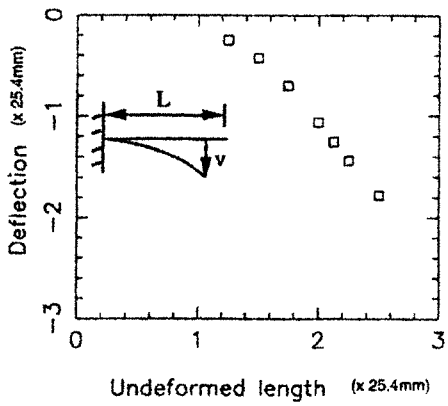

Fig. 6 Deflection at the free end of the strip under its own weight.

3.3 Equilibrium

The surface charge and the stiffness effects of the conductive strip can be computed accurately by examining the subdomain in small sizes. However, the labor involved in solving Eqs. (7) and (9) increases rapidly as the number of subdomains increases. Thus our interest lies in determining a reasonable number of subdomains.

For surface charge computation, the conductive

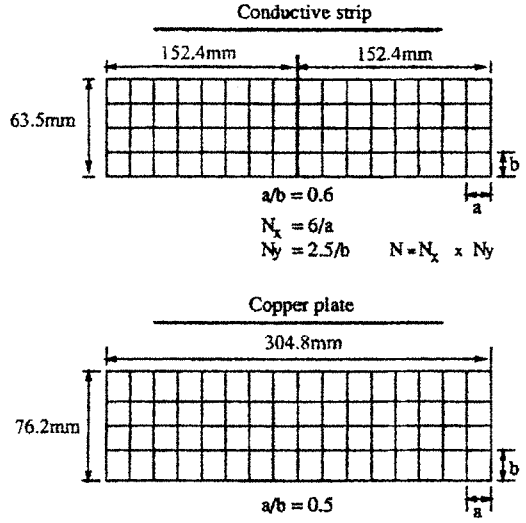

Fig. 7 Strip and copper plate divided into subdomains.

Table 1 Measurement of the flexural rigidity, $\bar{E}I$.

Measured point from root (mm)	Dimensionless displacement	Dimensionless load	Flexural rigidity kg. m^3/sec^2
38.1	0.2813	2.4210	0.421×10^{-6}
44.5	0.4005	3.6315	0.425×10^{-6}
50.8	0.5290	5.4210	0.425×10^{-6}
54.0	0.5582	6.5263	0.424×10^{-6}
57.2	0.6391	7.6842	0.427×10^{-6}

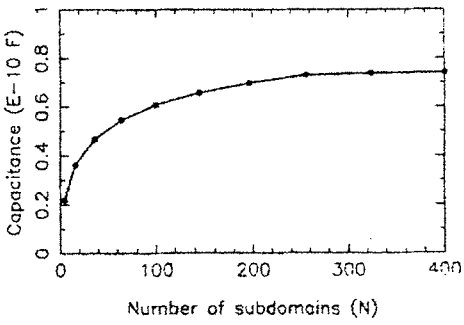

Fig. 8 Capacitance of the strip in terms of the number of subdomains.

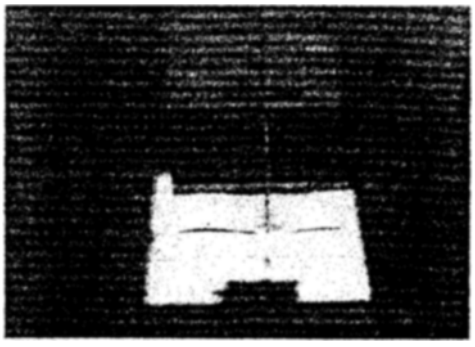

Fig. 9 Initial position of the strip before the system is charged.

strip is divided into N identical rectangular subdomains in which the dimensional ratio a/b is 0.6, and the copper plate is divided into 2N rectangular subdomains in which the dimensional ratio is 0.5 as shown in Fig. 7. Then, the surface charges at the equilibrium positions are predicted analytically by solving Eqs. (9) and (13) simultaneously. The associated capacitance is calculated by Eq. (9). Figure 8 shows the capacitance of the conductive strip in terms of the number of subdomains, in which the charge distributions are almost constant when the number of subdomains increases to more than 324 (N_x=36). The proper level of discretization is determined by examining these discretization effects.

Figures 9 and 10 show the initial position of the strip before wiring and the equilibrium position of the conductive strip after wiring, respectively. Figure 11 shows that the measured equilibrium positions compared favorally with the predicted shape of the strip.

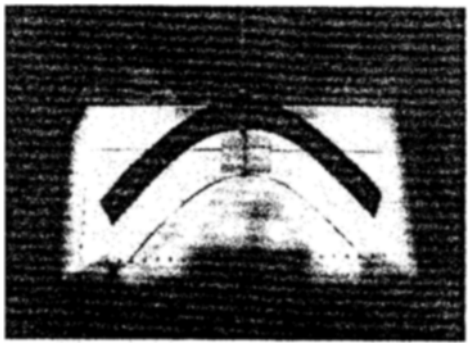

Fig. 10 Photograph of the equilibrium position of the strip (with 6000 volts).

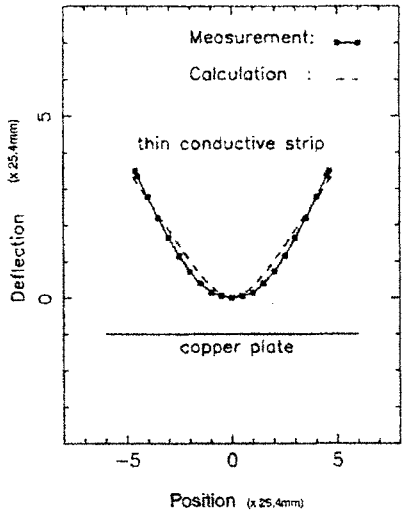

Fig. 11 Equilibrium position of the strip.

The gravitational effects and the effects of the grounded chamber (image charges) are neglected in the calculations. As shown in Fig. 11, the measured equilibrium positions agree with the analytically predicted equilibrium positions up to the tolerance of the measurement system. Errors may appear due to the exclusion effect of the grounded chamber, the boundary condition of the support of the strip, and the elastic anisotropy in the membranate.

Figure 12 shows different equilibrium positions depending on the applied potentials. As shown in Fig. 12, the deflections of the conductive strip increase as the applied potential increases.

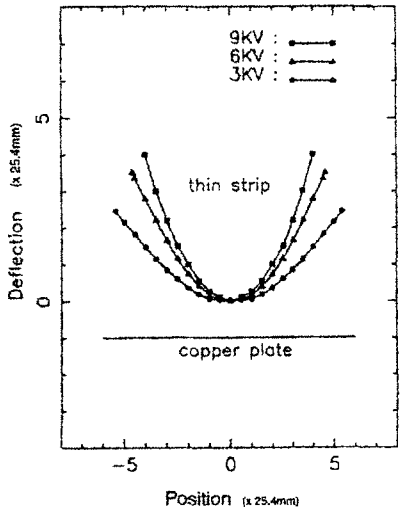

Fig. 12 Equilibrium position of the strip depending on the applied potential (volts).

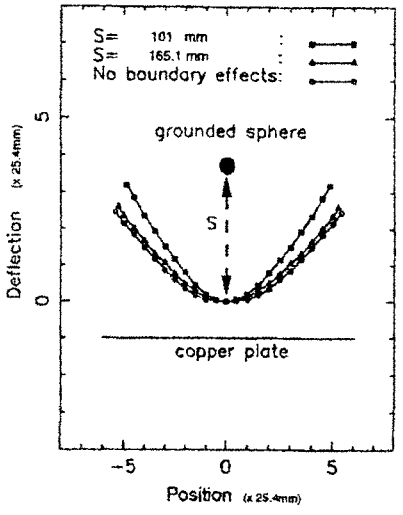

Fig. 14 Boundary effect of the grounded sphere (with 3000 volts).

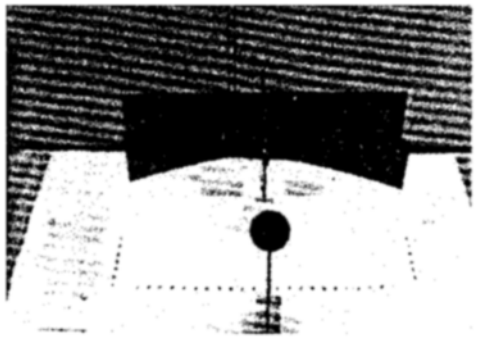

Fig. 13 Grounded sphere system.

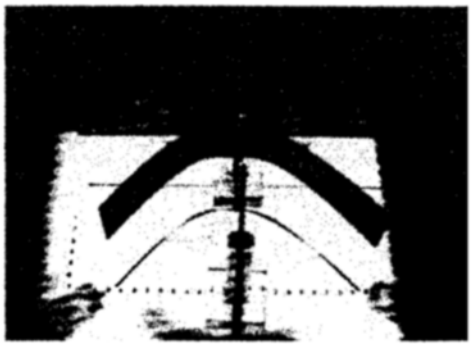

Fig. 15 Grounded copper rod system.

3.4 Boundary effects

Boundary effects are examined to seek efficient methods to get larger deflections of the strip using appropriate lower applied voltages. Two types of boundary effects, the effects of the grounded sphere (using a table tennis ball whose surface is coated with the conductive material Aquadag-E) and the grounded copper rod (using a same size of the copper rod fixed the strip) are examined in this experiment. The grounded sphere is positioned at the center line of the strip as shown in Fig. 13. The equilibrium positions are measured at varying distances s, between the strip and the grounded sphere using 3000 volts, as shown in Fig. 14. The deflection of the strip increases as the distance of the grounded sphere s becomes closer.

A grounded copper rod is positioned as shown

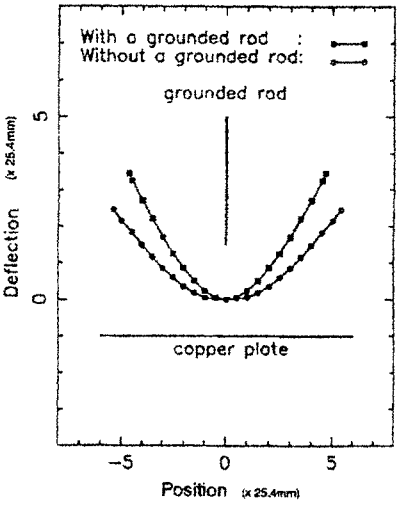

Fig. 16 Boundary effect of the copper rod (with 3000 volts).

in Fig. 15. Figure 16 shows that the grounded copper rod has an effect on the deflection of the strip, in which the deflection of the strip increases as the copper rod is positioned closer without any changes in the applied voltages. It implies that zero potentials are enforced by introducing negative induction charges on the surface of the grounded sphere or copper rod. The grounded elements can control the deflection of the strip depending on its position.

4. Conclusions

The objective of this paper is to examine various fundamental properties of planar electrodynamic structures, and to confirm the analytically predicted electrodynamic properties with experiments. The discretization effects associated with the charge distributions and the distributed displacements of the electrodynamic structure are examined for numerical calculations. The experiment is conducted in order to improve our understanding of discretization-based analysis of the fundamental characteristics of the electrodynamic structure. An experiment for the conductive strip is designed to measure the equilibrium positions when the conductive strip is wired. The deformations obtained experimentally agree with the predictions up to the tolerance of the measurement system. Grounded boundary effects dominate in the deflection of the conductive strip. In summary, the demonstrated ability to predict and to understand the behavior of these simple electrodynamic systems has important implications, one implication being that more complex electrodynamic structures can be designed and controlled using proper analyical methods.

References

Park, K., 1992, "An Investigation of Planar Electrodynamic Structures," Ph. D Dissertation, North Carolina State University, U. S. A.

Bryant, M. D. and Keltie, R. K., 1986, "A Characterization of the Linear and Nonlinear Dynamic Performance of a Practical Piezo-Electric Actuator," Sensors and Actuator, Vol. 1

Rhim, W. K., Collener, M. T., Simms, W. T., and Elleman, D. D., 1985, "Development of an Electrostatic Positioner for Space Material Processing," Rev. Sci. Instrum., 56(2), pp. 307 ~316

Udd, E., 1985, "Fiber-Optic Sensors in Space Applications," presented at NASA's InSpace Research Technology Workshop, Williamsburg, Virginia, U. S. A.

Mihora, D. J., Redmond, P. J., Crawford, R. F., and Mortz, M. S., 1979, "Electrostatically Formed Antennas (Test Concept)," NASA CR-159068

Brook, A. L., Coyner, J. V., Gardner, W. J., and Mihora, D. J., 1982, "Conceptual Design and Analysis of a Large Antenna Utilizing Electrostatic Membranate Management," NASA CR -3522

Golsee, J. W., Hinson, W. F., and Davis, W. T., 1985, "Electrostatic Forming and Testing of Polymer Films on a 16-foot Diameter Test Fixture," NASA Technical Memorandum 86328, Feb.

Grohe, W., 1960, Precision Measurement and Gaging Techniques Chemical Publishing Co., NY.

Lewis, R., 1985, "Solid-State Cameras," Electronic Imaging, Vol. 4, No. 1, pp. 45~52

Giachino, J. M., 1986, "Smart Sensors," Sensors and Actuators, Vol. 10, No. 3-4, pp. 239 ~248.

Kind, D. and Karner, H., 1985, High Voltage Insulation Technology, Friedr. Vieweg and Sohr Verlagsgesellshaft, Braunschweig.

Doggett, W. O., and Silverberg, L., 1990, "Protective chamber for Electrodynamic Experiments; Safety Measures and Operation Procedures," North Carolina State University, Internal Report.

Quinn, G. A., 1985, "High Accuracy Rotary and Linear Induction Position Transducers," Farrand Controls, Division of Farrand Industries, Inc., Valhalla, NY

Wada, B. K., 1989, "Adaptive structures," ASME AD-Vol. 15, ASME, NY

Kang, S. J. and Park, K., 1999, "Planar Dynamics of the Electric Charged Particles," J. of

The Korean Society for Noise and Vibration Engineering, Vol. 9, No. 3, pp. 621~628

Kang, S. J. and Park, K., 1999, "A Discrete-Particle Formulation of the Equations of Motion for Planar Electrodynamic Systems," KSME International Journal, The Korean Society of Mechanical Engineers, Vol. 13, No. 11, pp. 836~841

Harrington, R. F., 1968, Field Computation by Moment Methods, macmillan Co., NY, pp. 24~28.

Meirovitch, L., 1970, Methods of Analytical Dynamics, McGraw Hill Book Co., NY, pp. 161~170.

Meirovitch, L., 1980, Computational Methods in Structural Dynamics, Sijthoff & Noordhoff, pp. 230~238.

Carhahand, B. H., Luther, H. A. and Wilkes, J. O., 1969, Applied Numerical Methods, John Willey & Sons, Inc., NY, pp. 319~330.

Rao, S. M., Glisson, A. W., Wilton, D. D. and Vilula, B. S., 1979, "A Simple Numerical Solution Procedure for Static Problems Involving Arbitrary-Shaped Surfaces," IEEE Tran. on Antennas and Propagation, Vol. AP-27, No. 5, Sep. pp. 604~607.

Halliday, D. and Resnick, R., 1970, Fundamentals of Physics, John Wiley & Sons, Inc., Ch. 22-26

Yang, T. Y., 1973, "Matrix Displacement Solution to Elastica Problems of Beams and Frames," Int. J. Solids Structures, Vol. 9, pp. 829~842.

Scott, W. T., 1966, The Physics of Electricity and Magnetism, John Willey Sons Inc., NY

Smythe, W. R., 1950, Static and Dynamic Electricity, McGraw Hill Book Co., NY, pp. 4~5.